Self-Assembly Hot Paper

Deutsche Ausgabe: DOI: 10.1002/ange.201509233
Internationale Ausgabe: DOI: 10.1002/anie.201509233

Two-Dimensional Nanoporous Networks Formed by Liquid-to-Solid Transfer of Hydrogen-Bonded Macrocycles Built from DNA Bases

Nerea Bilbao, Iris Destoop, Steven De Feyter, and David González-Rodríguez**

Abstract: *We present an approach that makes use of DNA base pairing to produce hydrogen-bonded macrocycles whose supramolecular structure can be transferred from solution to a solid substrate. A hierarchical assembly process ultimately leads to two-dimensional nanostructured porous networks that are able to host size-complementary guests.*

Self-assembly provides the guidelines for engineering two-dimensional (2D) molecular networks on flat surfaces.[1] Those presenting void spaces, so-called "2D porous networks",[2] are especially interesting as they offer the possibility of immobilizing, in a repetitive and ordered way, different functional guest units that are complementary in size and shape. Such networks can be produced from the deposition of persistent covalent macrocycles.[3] The pore size and shape are thus predefined during synthesis, but this approach can be tedious and time-consuming if tunable systems that allow for small pore modifications are to be produced. A more appealing alternative is the generation of lattices with regular cavities from small monomers that, once on the surface, interact through weaker noncovalent bonds.[4] Upon physisorption, several degrees of translational, rotational, and vibrational freedom are lost, and as a result, molecules that display very weak and ill-defined binding in solution can form well-ordered, yet dynamic assemblies that are held together by multiple supramolecular interactions when confined in two dimensions. However, although much has been learned over the last years, this second approach suffers from the limitation that the kind of network attained cannot always be reliably predicted, as it depends on a subtle interplay between molecule–molecule, molecule–solvent, and molecule–substrate interactions.

An intermediate and ideal situation would be reached in the case of macrocycles that are assembled in solution through reversible noncovalent interactions,[5] but are robust enough to survive as well-defined, monodisperse species after transfer from solution to a substrate. These are indeed highly challenging requirements for self-assembled macrocycles as the self-assembly rules change drastically when molecules are concentrated on a surface. On the one hand, intra- and intermolecular binding events are compensated, and chelate cooperativity, the key factor promoting cycle formation in dilute solutions, becomes less important. On the other hand, physisorbed molecules generally tend to maximize molecule–substrate interactions, so that networks with empty spaces are usually avoided if an alternative, more densely packed lattice can be accessed. All of these issues ultimately result in a low-fidelity liquid-to-substrate transfer of supramolecular information. In other words, self-assembly in solution is typically not reproduced on the surface and vice versa.

Herein, we present a bioinspired approach that makes use of DNA base[1g] pairing to produce tunable macrocycles (Figure 1) in solution whose supramolecular identity is reliably transferred to highly oriented pyrolytic graphite (HOPG), ultimately yielding ordered 2D porous networks by a hierarchical self-assembly process. This was accomplished by rational design of the molecular structure. First, we reasoned that such cyclic systems should be endowed with high intermolecular association constants and effective molarities (thus leading to strong chelate effects), which must stem from an optimal monomer preorganization towards a specific cycle size.[2c] Second, to produce robust, highly ordered 2D networks, selective and directional inter-macrocycle interactions, of a secondary hierarchy level, should be promoted. Third, the generation of unique and uniform nanopores, whose dimensions would be precisely defined by the macrocycle cavity, must come from dense

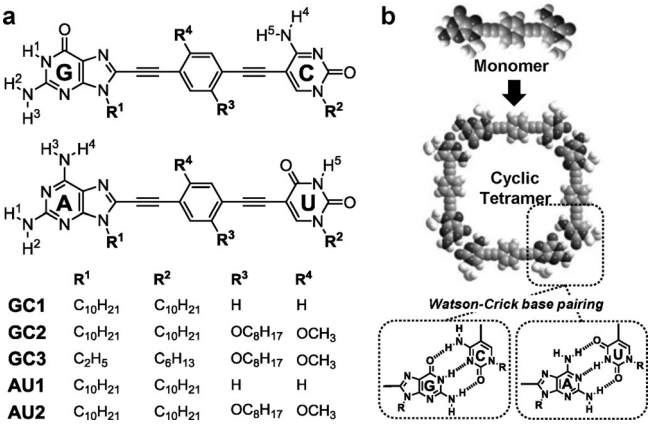

	R^1	R^2	R^3	R^4
GC1	$C_{10}H_{21}$	$C_{10}H_{21}$	H	H
GC2	$C_{10}H_{21}$	$C_{10}H_{21}$	OC_8H_{17}	OCH_3
GC3	C_2H_5	C_6H_{13}	OC_8H_{17}	OCH_3
AU1	$C_{10}H_{21}$	$C_{10}H_{21}$	H	H
AU2	$C_{10}H_{21}$	$C_{10}H_{21}$	OC_8H_{17}	OCH_3

Figure 1. a) Structure of the monomers **GC1**–**GC3** and **AU1**–**AU2**. b) Square-shaped cyclic tetramers are assembled by Watson–Crick G-C/A-U H-bonding.

[*] N. Bilbao, Dr. D. González-Rodríguez
Nanostructured Molecular Systems and Materials Group
Departamento de Química Orgánica, Facultad de Ciencias
Universidad Autónoma de Madrid
28049 Madrid (Spain)
E-mail: david.gonzalez.rodriguez@uam.es
I. Destoop, Prof. S. De Feyter
Division of Molecular Imaging and Photonics
Department of Chemistry, KU Leuven–University of Leuven
Celestijnenlaan 200 F, 3001 Leuven (Belgium)
E-mail: steven.defeyter@chem.kuleuven.be

Supporting information for this article is available on the WWW under http://dx.doi.org/10.1002/anie.201509233.

networks where any secondary unspecific pores are filled by a rational positioning of peripheral tails. In this way, additional stabilizing interactions with the substrate are also established, so that any other competing intermolecular arrangement is eluded. Furthermore, we demonstrate that the resulting 2D nanostructured porous lattices, which were studied by scanning tunneling microscopy (STM) at the solvent–HOPG interface, are able to selectively host size-complementary guests in a controlled and reproducible fashion.

Monomer design (**GC1**–**GC3** and **AU1** and **AU2**,[6,7] Figure 1a) was based on a π-conjugated *para*-diethynylbenzene unit substituted with complementary nucleobases at the edges: guanine (G) and cytosine (C) or 2-aminoadenine (A) and uracil (U). This rigid and linear structure, together with the 90° angle provided by Watson–Crick pairing, resulted in the quantitative formation of unstrained square-shaped tetrameric assemblies (Figure 1b) over a broad concentration, temperature, and solvent-polarity range, as previously demonstrated by us in solution experiments (see also the Supporting Information, Figure S1).[8] The exceptional stability, which was particularly evident for the G-C couple, was ascribed to the strong chelate effect measured upon cyclotetramerization, which originates mainly from the optimally preorganized monomer structure.

We initiated our studies with monomers **GC1** and **AU1**, both equipped with bases with long decyl tails. Despite our efforts, ordered networks could not be imaged when these monomers were deposited onto HOPG in a variety of solvents at concentrations of 10^{-4}–10^{-6} M. The only exception was **GC1** in a 1,2,4-trichlorobenzene (TCB)/octanoic acid (OA; 1:1) mixture. When a 5.0×10^{-6} M solution of **GC1** was drop-casted onto freshly cleaved HOPG, large organized domains of non-cyclic oligomers were obtained (Figure 2a). The models suggested that instead of establishing the expected Watson–Crick interactions, the ditopic π-conjugated monomers were arranged in parallel rows comprising packed pairs of molecules[9] that were associated by H-bonding interactions between the G carbonyl group and the C amino H4 proton (Figure 2b). At the same time, the rows grow by additional H-bonding between the C carbonyl group and the G H1 and G H2 protons. Although not clearly observed in the images, such a double-chain pattern leaves all of the peripheral long alkyl tails lying flat on the surface and arranged orthogonally with respect to the rows, so that they can establish multiple van der Waals interactions to stabilize the network. Furthermore, we believe that OA solvent molecules might also participate in the network by establishing H-bonding interactions with the nucleobases and van der Waals interactions with the alkyl tails between rows (see Figure S2). As a matter of fact, the use of this solvent was essential to properly solubilize the samples and to reproduce this pattern; in its absence, no ordered networks were obtained. **GC1** is an interesting example as even though it can form macrocyclic assemblies in solution (Figure S1), it is then reorganized on HOPG to yield a more densely packed network, with a density calculated as 228.0 g mol^{-1} nm^{-2}. Cyclic **GC1** or **AU1** assemblies are probably not preserved on the surface because they leave large void spaces, 2.2 nm in diameter, that would lead to lower-density networks, with an estimated density of 180.3 g mol^{-1} nm^{-2}.[6] Hence, we reasoned that partial filling of the cavities with alkyl tails, introduced at the central benzene block (as in **GC2** and **AU2**), might be a strategy to increase surface density and favor the formation of cyclic tetramer networks.

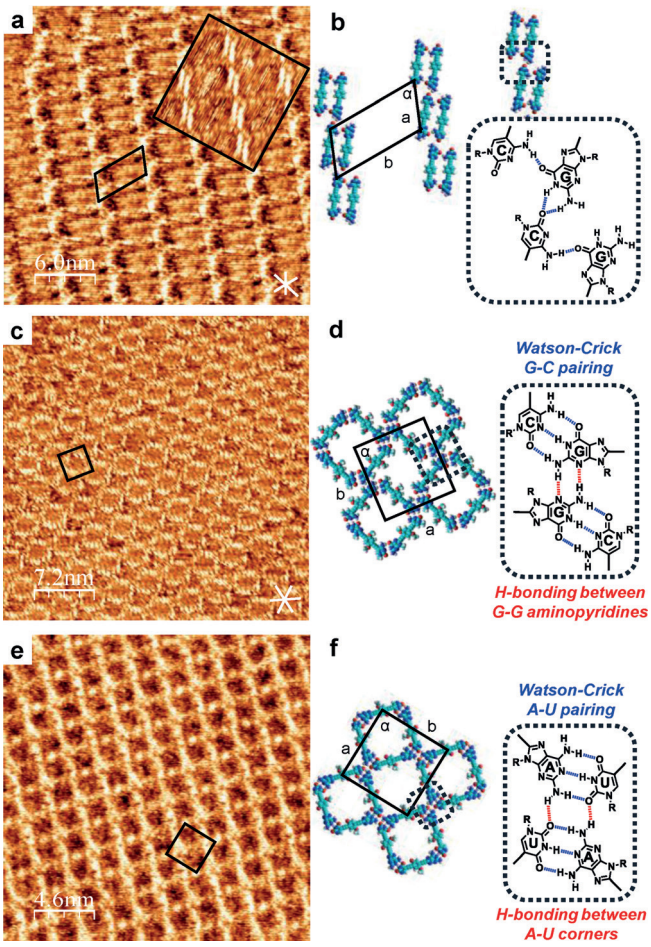

Figure 2. a) High-resolution STM image of **GC1** on HOPG from a solution of **GC1** (5.0×10^{-6} M) in TCB/OA (1:1; tunneling parameters: $I_{set}=50$ pA, $V_{bias}=-350$ mV). The inset, showing the arrangement in monomer pairs, corresponds to another STM image on HOPG from a **GC1** solution (6.0×10^{-6} M) in TCB/OA (1:1; $I_{set}=50$ pA, $V_{bias}=-350$ mV). b) Model for **GC1**. The unit cell is indicated by black lines: $a=2.7\pm0.1$ nm; $b=4.5\pm0.1$ nm; $\alpha=68\pm1°$. c) High-resolution STM image of **GC2** on HOPG from a solution of **GC2** (7.1×10^{-6} M) in OA ($I_{set}=280$ pA, $V_{bias}=-180$ mV). d) Model for **GC2**: $a=3.4\pm0.1$ nm; $b=3.6\pm0.1$ nm; $\alpha=92\pm2°$. e) High-resolution STM image of **AU2** on HOPG from a solution of **AU2** (7.9×10^{-5} M) in TCB/OA (1:1; $I_{set}=100$ pA, $V_{bias}=-350$ mV). f) Proposed model for **AU2**: $a=3.5\pm0.1$ nm; $b=3.5\pm0.1$ nm; $\alpha=91\pm1°$. White lines indicate the normal axes of graphite.

When TCB/OA (0:1 or 1:1) solutions of **GC2** or **AU2** (10^{-5}–10^{-6} M) were applied onto HOPG, large domains of cyclic tetrameric species were now successfully imaged (Figure 2c,e and S3). Interestingly, STM reveals that these networks are mainly stabilized by two sets of H-bonding motifs of different hierarchy. First, strong G-C/A-U Watson–Crick triple H-bonding, leading to the observed square-shaped motifs, is conserved on the surface. These discrete

tetramers then pack in 2D by establishing secondary interactions between H-bonding donor and acceptor groups that do not participate in Watson–Crick pairing. However, these interactions are different for **GC2** and **AU2** and thus lead to distinct network arrangements, as previously shown for other H-bonded systems.[1h] In the first case, G-G double H-bonding interactions between aminopyridine-type fragments (Figure 2d) are established, leading to regular lattices in which the rings interact through their G edges. On the contrary, for **AU2**, the square-shaped cycles bind through their corners by establishing H-bonding interactions between the A H2 proton and the external U carbonyl lone pair (Figure 2f), so that the resulting network appears as a continuous grid. It should be noted that **GC2** and **AU2** could in principle establish any of these two secondary H-bonding configurations (see Figure S4), but these distinct centrosymmetric lattice arrangements were always observed for each molecule under different concentration conditions, and annealing or time-dependent studies (Figure S5) did not show any network reorganization, suggesting that they constitute equilibrium states. Both the **GC2** and **AU2** networks leave secondary pores between the cyclic tetramers that have a size comparable to that defined by the macrocyclic cavity where the external alkyl tails of the nucleobases are forced to group. However, the proposed models show that the C_{10} alkyl chains in each **GC2**/**AU2** base do not fit properly into the space left between four cyclic tetramers. Despite their high affinity for the HOPG substrate, some of these chains must necessarily desorb and back-fold towards the supernatant solution. This is an energetically unfavorable situation that indicates that secondary H-bonding interactions between tetramers dominate over van der Waals interactions in the stabilization of the networks. The interaction between corners leaves secondary pores that are significantly larger (5.6 nm^2) than those generated by the interaction between purine edges (3.4 nm^2), where the long peripheral tails should fit better and establish stronger interactions with the substrate. As a matter of fact, larger and better-ordered domains were observed for **AU2**, for which the surface density was calculated to be 232.1 $g\,mol^{-1}\,nm^{-2}$, than for **GC2** (see Figure S5).[10]

In view of these results, we decided to further optimize the GC cyclic tetramer network and synthesize a third-generation monomer (**GC3**), which is equipped with shorter C_2 and C_6 chains at the G and C bases, respectively. The length of these alkyl chains was precisely tailored for each base to completely fill the secondary unspecific pores generated between four cyclic tetramers and, at the same time, to allow the whole length of the chains to physisorb onto HOPG, thus promoting additional interactions to stabilize the network. When **GC3** solutions in 1:1 TCB/OA were drop-casted onto HOPG, large domains of cyclic tetrameric species were again observed by STM (Figure 3a and S5). In this case, the macrocycle network, the density of which was now calculated as 247.7 $g\,mol^{-1}\,nm^{-2}$, showed a higher stability at the solid–liquid interface, and as a result, excellent coverage and a superior monolayer resolution were attained (Figure 3b). In some images with higher resolution, ill-defined features of bright contrast (though darker than the π-conjugated skeleton) were

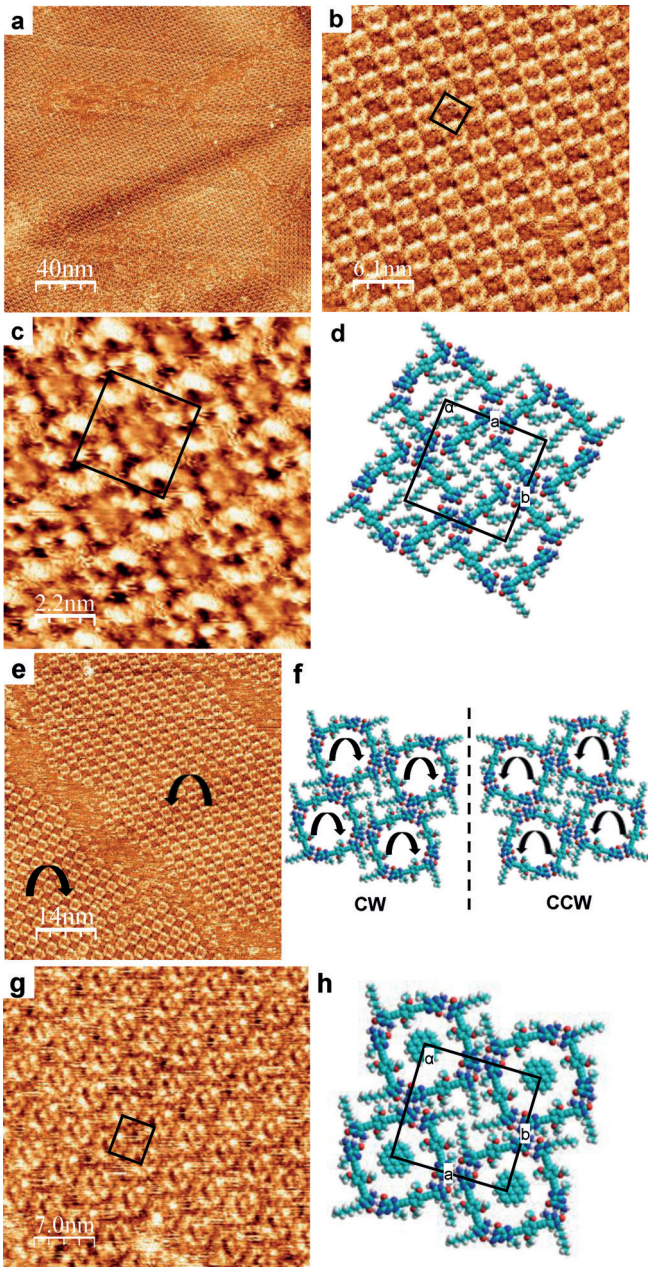

Figure 3. a, b) STM images of **GC3** on HOPG from a solution of **GC3** (8.2×10^{-6} M) in TCB/OA (1:1; $I_{set}=200$ pA, $V_{bias}=-300$ mV). c) High-resolution STM image of **GC3** on HOPG from a solution of **GC3** (8.2×10^{-6} M) in TCB/OA (1:1; $I_{set}=200$ pA, $V_{bias}=-300$ mV). d) Model for **GC3**: $a=b=3.6\pm0.1$ nm; $\alpha=89\pm1°$. e) STM image of **GC3** showing two domains with different pore chiralities (f). g) STM image of the **GC3**/**cor** bicomponent system at the HOPG–TCB/OA (1:1) interface ($I_{set}=80$ pA, $V_{bias}=-350$ mV). h) Model for this host–guest system: $a=3.6\pm0.1$ nm; $b=3.5\pm0.2$ nm; $\alpha=89\pm1°$.

observed within and between the pores (Figure 3c), which we assigned to the inner and outer alkyl tails, as depicted in the model in Figure 3d. The growth of the domains, driven by thermodynamics, could be observed with time along consecutive scans until large, single domains, whose size may extend well beyond 100×100 nm^2 (Figure S5), were obtained. The **GC3** (and also **GC2**) domains consisted of cyclic tetramers

with the same surface chirality (Figure 3e and S6).[11] This chirality depends on the side of the macrocycle that is in contact with the substrate. Assuming an arbitrary cycle sense taking the Watson–Crick H-bonding interaction from G to C, we could define clockwise (CW) and counter-clockwise (CCW) tetramer configurations on the surface (Figure 3f and S6).

To confirm the ability of our nanostructured porous surface to host size-complementary molecules, mixtures of **GC1**–**GC3** and matching π-conjugated planar guests, namely coronene (**cor**), were co-deposited and imaged by STM at the solid–liquid interface. Premixed solutions of the monomer with an excess of guest were prepared in TCB/OA (1:1) and drop-casted onto HOPG.[6] The mixtures consistently led to surface networks that appeared to be very different to those obtained in the absence of guests (according to STM analysis, compare Figure 3b, g). Medium-sized domains covering large areas were observed, and bright features are now localized inside the cavities, which constitutes strong evidence for the co-adsorption of **cor** molecules (see also Figure S7 and S8). According to the models, the smaller host fits properly into the cyclic tetramer cavity, but it must compete for the pore with the C_8H_{17} chains attached to the central block. We propose that these inner chains are back-folded in the supernatant solution to leave room for the guest molecules, which can then establish strong interactions with HOPG. At the domain borders, fuzzy areas that cannot be resolved on the timescale of the scanning microscope were observed, which may be evidence of this adsorption/desorption equilibrium between the C_8H_{17} chains and **cor** (Figure S8B). We believe that **cor** inclusion results from an energy-minimized packing to achieve maximum density. Independent **cor** islands were never observed, even when a large excess of guest molecules was used. The high-contrast central features were only observed when both host and guest are transferred together from the solution onto HOPG, and never when an excess of **cor** was added to a preformed **GC3** cyclic tetramer network. This result seems to indicate that the **GC3** porous network, which features adsorbed C_8H_{17} chains, is kinetically stable enough to impede **cor** physisorption.

In summary, we have described a novel strategy based on molecular self-assembly towards unconventional 2D nanoporous systems. Our approach differs from previous H-bonded lattices where the porous network is built on the surface by making use of weak interactions between di- or tritopic molecules, the phthalic or trimesic acids being representative examples. Here, robust macrocycles were assembled by making use of Watson–Crick interactions between DNA bases, and their supramolecular structures could be preserved upon transfer to a surface. Chiral domains are then assembled by the establishment of multiple and distinct H-bonding interactions of a second-order hierarchy between tetrameric macrocycles. The ability of the nanoporous network to host size-complementary guests was preliminarily demonstrated, and stable bimolecular assemblies with coronene were reproducibly obtained. A large number of possibilities for modular surface nanostructuring are now conceivable.

Acknowledgements

Funding from the European Union (ERC Starting Grant 279548), MICINN (CTQ2014-57729-P), the Fund for Scientific Research—Flanders, KU Leuven (GOA 11/003), the Belgian Federal Science Policy Office (IAP-7/05), and the European Research Council (FP7/2007–2013, ERC Grant Agreement 340324) is gratefully acknowledged. We thank Dr. Oleksandr Ivasenko and Dr. Kunal S. Mali for useful discussions and advice.

Keywords: macrocycles · porous networks · self-assembly · supramolecular chemistry · surface assembly

How to cite: *Angew. Chem. Int. Ed.* **2016**, *55*, 659–663
Angew. Chem. **2016**, *128*, 669–673

[1] a) J. V. Barth, G. Costantini, K. Kern, *Nature* **2005**, *437*, 671–679; b) F. Cicoira, C. Santato, F. Rosei, *Top. Curr. Chem.* **2008**, *285*, 203–267; c) J. A. A. W. Elemans, S. Lei, S. De Feyter, *Angew. Chem. Int. Ed.* **2009**, *48*, 7298–7332; *Angew. Chem.* **2009**, *121*, 7434–7469; d) A. Ciesielski, C.-A. Palma, M. Bonini, P. Samori, *Adv. Mater.* **2010**, *22*, 3506–3520; e) L. Bartels, *Nat. Chem.* **2010**, *2*, 87–95; f) R. Otero, J. M. Gallego, A. L. Vázquez de Parga, N. Martín, R. Miranda, *Adv. Mater.* **2011**, *23*, 5148–5176; g) M. El Garah, R. C. Perone, A. Santana Bonilla, S. Haar, M. Campitiello, R. Gutiérrez, G. Cuniberti, S. Masiero, A. Ciesielski, P. Samori, *Chem. Commun.* **2015**, *51*, 11677–11680; h) P. Zalake, K. G. Thomas, *Langmuir* **2013**, *29*, 2242–2249.

[2] a) T. Kudernac, S. Lei, J. A. A. W. Elemans, S. De Feyter, *Chem. Soc. Rev.* **2009**, *38*, 402–421; b) K. S. Mali, J. Adisoejoso, E. Ghijsens, I. De Cat, S. De Feyter, *Acc. Chem. Res.* **2012**, *45*, 1309–1320; c) T. Kudernac, A. K. Mandal, J. Huskens, *Langmuir* **2015**, *31*, 157–163.

[3] a) C. Safarowsky, L. Merz, A. Rang, P. Broekmann, B. A. Hermann, C. A. Schalley, *Angew. Chem. Int. Ed.* **2004**, *43*, 1291–1294; *Angew. Chem.* **2004**, *116*, 1311–1314; b) S. Yoshimoto, K. Suto, A. Tada, N. Kobayashi, K. Itaya, *J. Am. Chem. Soc.* **2004**, *126*, 8020–8027; c) E. Mena-Osteritz, P. Bäuerle, *Adv. Mater.* **2006**, *18*, 447–451; d) K. Tahara, J. Gotoda, C. N. Carroll, K. Hirose, S. De Feyter, Y. Tobe, *Chem. Eur. J.* **2015**, *21*, 6806–6816.

[4] a) S. Stepanow, M. Lingenfelder, A. Dmitriev, H. Spillmann, E. Delvigne, N. Lin, X. Deng, C. Cai, J. V. Barth, K. Kern, *Nat. Mater.* **2004**, *3*, 229–233; b) K. Tahara, S. Furukawa, H. Uji-i, T. Uchino, T. Ichikawa, J. Zhang, W. Mamdouh, M. Sonoda, F. C. De Schryver, S. De Feyter, Y. Tobe, *J. Am. Chem. Soc.* **2006**, *128*, 16613–16625; c) M. O. Blunt, J. C. Russell, M. D. Giménez-Lopez, J. P. Garrahan, X. Lin, M. Schröder, N. R. Champness, P. H. Beton, *Science* **2008**, *322*, 1077–1081; d) W. Xu, J. Wang, M. F. Jacobsen, M. Mura, M. Yu, R. E. A. Kelly, Q. Meng, E. Lægsgaard, I. Stensgaard, T. R. Linderoth, J. Kjems, L. N. Kantorovich, K. V. Gothelf, F. Besenbacher, *Angew. Chem. Int. Ed.* **2010**, *49*, 9373–9377; *Angew. Chem.* **2010**, *122*, 9563–9567.

[5] M. J. Mayoral, N. Bilbao, D. González-Rodríguez, *ChemistryOpen* **2015**, DOI: 10.1002/open.201500171.

[6] See the Supporting Information for further details.

[7] a) J. Camacho-García, C. Montoro-García, A. M. López-Pérez, N. Bilbao, S. Romero-Pérez, D. González-Rodríguez, *Org. Biomol. Chem.* **2015**, *13*, 4506–4513; b) N. Bilbao, V. Vázquez-González, M. Aranda, D. González-Rodríguez, *Eur. J. Org. Chem.* **2015**, *32*, 7160–7175.

[8] a) C. Montoro-García, J. Camacho-García, A. M. López-Pérez, N. Bilbao, S. Romero-Pérez, M. J. Mayoral, D. González-

Rodríguez, *Angew. Chem. Int. Ed.* **2015**, *54*, 6780 – 6784; *Angew. Chem.* **2015**, *127*, 6884 – 6888; b) S. Romero-Pérez, J. Camacho-García, C. Montoro-García, A. M. López-Pérez, A. Sanz, M. J. Mayoral, D. González-Rodríguez, *Org. Lett.* **2015**, *17*, 2664 – 2667; c) C. Montoro-García, J. Camacho-García, A. M. López-Pérez, M. J. Mayoral, N. Bilbao, D. González-Rodríguez, *Angew. Chem. Int. Ed.*, DOI: 10.1002/anie.201508854; *Angew. Chem.*, DOI: 10.1002/ange.201508854.

[9] Similar 2D arrangements were observed for other structurally related ditopic monomers; see: A. Llanes-Pallas, M. Matena, T. Jung, M. Prato, M. Stöhr, D. Bonifazi, *Angew. Chem. Int. Ed.* **2008**, *47*, 7726 – 7730; *Angew. Chem.* **2008**, *120*, 7840 – 7844.

[10] However, the reasons why **GC2** tetramers prefer to bind through the purine edges are still not clear. Our hypothesis, developed in Figure S4, is that this particular arrangement may be a consequence of short-range cancelation of the nucleobase dipole moments, which are much stronger in the G-C pair than in the A-U pair; see: J. Sponer, J. Leszczynski, P. Hobza, *Biopolymers* **2001**, *61*, 3 – 31.

[11] a) L. Pérez-García, D. B. Amabilino, *Chem. Soc. Rev.* **2007**, *36*, 941 – 967; b) J. Elemans, I. De Cat, H. Xu, S. De Feyter, *Chem. Soc. Rev.* **2009**, *38*, 722 – 736.

Received: October 2, 2015
Published online: November 24, 2015

